eprints@whiterose.ac.uk
https://eprints.whiterose.ac.uk/

PCCP

Photo-Induced Oxidation of the Uniquely Liganded Heme *f* in the Cytochrome *b₆f* Complex of Oxygenic Photosynthesis

Adrien A. P. Chauvet,[a][*][†] Rachna Agarwal,[b] André al Haddad,[a] Frank van Mourik[a] and William A. Cramer[b]

The ultrafast behavior of the ferrous heme *f* from cytochrome *b₆f* complex of oxygenic photosynthesis is revealed by means of transient absorption spectroscopy. Benefiting from the use of microfluidic technologies for handling the sample as well as from a complementary frame-by-frame analysis of the heme dynamics, the different relaxation mechanisms from vibrationally excited states are disentangled and monitored via the shifts of the heme *α*-absorption band. Under 520 nm laser excitation, about 85 % of the heme *f* undergoes pulse-limited photo-oxidation (< 100 fs), with the electron acceptor being most probably one of the adjacent aromatic amino acid residues. After charge recombination in 5.3 ps, the residual excess energy is dissipated in 3.6 ps. In a parallel pathway, the remaining 15 % of the hemes directly relax from their excited state in 2.5 ps. In contrast to a vast variety of heme-proteins, including the homologous heme c_1 from the cytochrome bc_1 complex, there is no evidence that heme *f* photo-dissociates from its axial ligands. Due to its unique binding, with histidine and an unusual tyrosine as axial ligands, the heme *f* exemplifies a dependence of ultrafast dynamics on the structural environment.

Introduction

The cytochrome (cyt) b_6f complex plays a central role in the oxygenic photosynthetic apparatus of all plants, green algae, and cyanobacteria. It mediates electron transport between the photosystem I and II reaction center complexes while creating an electrochemical gradient across the thylakoid membrane.[1] The electrochemical potential gradient that is generated provides the free energy for ATP synthesis, the universal energy currency in living organisms. The overall structure and physiological functions of the cyt b_6f complex are similar to its homologue cyt bc_1 in mitochondria and photosynthetic bacteria. [2, 3] Cyt b_6f is, however, more complex as it contains additional prosthetic groups i.e. one molecule each of β-carotene (Car), chlorophyll *a* (Chl *a*) and an additional c-type heme, called heme c_n, on the electrochemically negative (n) side of the complex in each monomer (Figure 1).[1] The b_6f complex has a symmetric dimeric structure in which the monomer is comprised of five key components that are directly involved in the electron transport pathway:
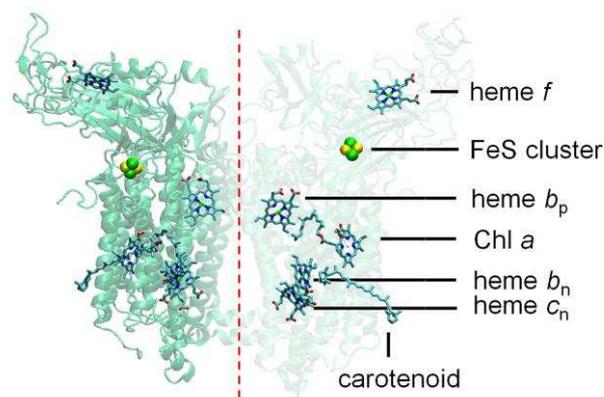
Figure 1: Backbone structure and prosthetic groups of the cytochrome b6f complex. The crystallographic data is taken from the 2E74.pdb file.[4]

(1) Heme *f* which is located in the thylakoid lumen and serves as electron donor for the reduction of plastocyanin, or of cytochrome *c* under environmental conditions of low copper content.

(2) The Rieske [2Fe-2S] iron-sulfur cluster which mediates electron transfer between the quinol at the Q_p (quinone binding site on the electrochemically positive side of the membrane) site and heme f via a series of conformational changes.[5, 6]

(3, 4) Hemes b_n and b_p on the electrochemically negative and positive sides of the membrane mediate electron transfer between the quinone binding sites, Q_n and Q_p, respectively;[1]

(5) Heme c_n, which is ligated within 4Å of a propionate of

a. *Ecole Polytechnique Fédérale de Lausanne (EPFL), Laboratoire de Spectroscopie Ultrarapide (LSU), ISIC, Faculté des Sciences de Base and Lausanne Centre for Ultrafast Science (LACUS), Station 6, 1015 Lausanne, Switzerland.*

b. *Purdue University, Department of Biological Sciences, West Lafayette, Indiana 47907, United States.*

* **Corresponding Author:** adrien.chauvet@gmail.com

† **Present Addresses:** Université de Genève, GAP-Biophotonics, Chemin de Pinchat 22, CH-1211 Geneva 4, Switzerland.

Electronic Supplementary Information (ESI) available: Heme *f* signal extraction; Fitting procedure; Fitting results. See DOI: 10.1039/x0xx00000x

heme b_n,[7-9] is a major component of the n-side electron transfer pathway.[10] Possible functions for the additional β-carotene (Car) and Chlorophyll a (Chl a) molecule present in each monomer of the complex (Figure 1) have been discussed.[11-13]

As in the organization of heme c_1 in the cyt bc_1 complex, heme f in the b_6f complex is covalently attached to the protein by two cysteinyl residues. However, the heme f has as axial ligands a tyrosine (Tyr 1) and a histidine (His 26) (Figure 2) instead of a methionine (Met) and a histidine (His) as is the case in cyt bc_1.[14] The axial ligands of heme f are unusual as the Tyr 1 ligation utilizes the N-terminal amino acid of the cytochrome polypeptide. This structural specificity confers the heme f with unique ultrafast dynamics.

The ultrafast behaviour, specifically, the relaxation of photo-excited hemes, has been the subject of extensive study.[15-17] Ultrafast analysis can describe the short-lived local electronic and nuclear modifications that underlie physiological processes, and can elucidate the initial mechanisms and local structural and electronic modifications that influence the functions of the protein complex. For example, the ultrafast response of the cyt bc_1 complex has recently been resolved. The study revealed that, while most ferrous heme-proteins undergo photo-dissociation of one of their axial ligands,[15, 17-21] the b-hemes in the cyt bc_1 complex undergo an unusual photo-induced oxidation.[20] The aim of the present study is to resolve the ultrafast response of the heme f in the cyt b_6f complex and to understand the effects of the unique binding configuration[14] on its ultrafast behaviour and the possible relation to its overall physiological function.

Similar to the approach taken in the previous work on cyt bc_1,[20] the present study also focuses on the α-band in the 550-560 nm spectral region rather than on the more intense Soret band as the Soret band is spectrally congested in the cytochrome b_6f complex due to the presence of multiple heme-types, as well as the Car and Chl a. Like the Soret band, the α-band is also sensitive to changes in the electronic state and coordination of the hemes. The α-band region consequently offers a clearer window for studying the ultrafast behaviours of the heme. The particularity of the present work not only reside in the monitoring of unusual photo-oxidation processes within heme-proteins, but also resides in the analytical method which is to complement common global exponential fitting of the data set by a detailed spectral fitting at each single time delay. Indeed, global fitting methods fall short when it comes to disentangling gradual spectral changes. However, successive spectral fitting of each data taken (spectrum at each delay times), even if based on particular models, allows to clearly resolve the dynamics of the band-shifts.

Material and Methods

Purification of Cytochrome b6f Complex: Active dimeric cytochrome b_6f complex was isolated from leaves of *Spinacea* as previously described.[22] Briefly ~400 g of baby spinach leaves
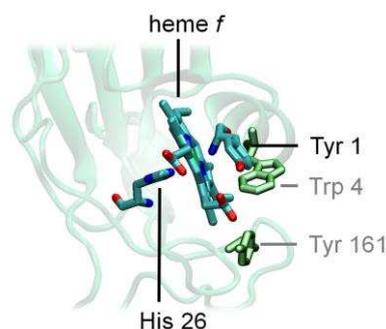
Figure 2: Structure of heme f showing the axial amino acid ligands, the N-terminal Tyr 1 and His 26 as well as additional aromatic residues closest to it (Trp 4 and Tyr 161 in *C.-reinhardtii*) as well as its axial amino acid ligands, the N-terminal Tyr 1 and His 26. The crystallographic data is taken from the 2E74.pdb file.[4]

in early growth phase were macerated in grinding buffer (Tris-HCl, 50 mM, pH 7.5; NaCl, 100 mM; sucrose 200 mM; protease inhibitors) at 4°C and the homogenate was filtered and centrifuged at 10,000 x g for 30 min (4°C) to obtain chloroplasts.The chloroplasts were osmotically shocked (10 mM Tris-HCl, pH 8.0 at 4°C, and protease inhibitors) and washed with 2 M NaBr (in Tris 10 mM, pH 8.0 at 4°C), and centrifuged at 10,000 x g for 30 min (4°C). The resulting pellet was resuspended in TNE-sucrose buffer (Tris-HCl 30 mM, pH 7.5, NaCl 50 mM, EDTA 1 mM, 10% sucrose and protease inhibitors). Detergent extraction was performed with 0.9% β–octyl glucoside and 0.1% sodium cholate at a chlorophyll-a concentration of 2 mg/ml for 25 minutes at room temperature. Insoluble material was removed by ultra-centrifugation at 300 000 x g for 45 min at 4°C. The supernatant was further enriched in cyt b_6f by precipitation of contaminating proteins with 35% ammonium sulfate and ultra-centrifugation at 300 000 x g for 20 min at 4°C. Cyt b_6f in the supernatant was purified by propyl-agarose hydrophobic column chromatography with 0.05% undecyl maltoside (UDM). Cyt b_6f monomer and dimer were separated by a 10-32% sucrose density gradient centrifugation [22]. Dimeric cyt b_6f complex was concentrated and the buffer exchanged to TNE-UDM (0.05%). The subunit composition of the b_6f preparation was assessed by SDS-PAGE, CN-PAGE, and redox difference spectra using standard procedures (data not shown). All assays were performed in 30 mM Tris-HCl (pH 7.5), 50 mM NaCl, 0.2 mM EDTA, and 0.04 % UDM. The electron transport activity of the dimeric complex, 150 -200 electrons/cyt f – sec, was assessed using decyl-plastoquinol as electron donor and *Chlamydomonas* plastocyanin as electron acceptor.[23]

Sample handling for kinetic measurements: The sample was housed in a microfluidic flow-cell, [24] while in aerobic conditions. In brief, the flow-cell requires a minimal sample volume of only ~250 µL that flows into a fixed square quartz silica capillary of 0.5-mm path-length and 0.25-mm thick window. The flow is generated by a flow-through friction based (turbisc) micro-pump from the Swiss Center for Electronics and Microtechnology (CSEM).[25] Enclosed bubbles are removed from the circuit via a decantation chamber. The generated flow of ~0.1 mL/s is sufficient to refresh the sample for each laser shot at 1 kHz repetition rate. The oxidation state

of the hemes as well as the possible degradation of the complexes is directly monitored by recording their steady-state absorbance through the white light continuum of the probe beam.

Transient absorption spectroscopy: The 800-nm output of a 1 kHz regenerative amplifier is used to pump a home-made visible non-collinear optical parametric amplifier (NOPA, see ref.[26] for a detailed description) producing the ~40 fs, 520-nm pump pulses with a full-width-half-maximum of 15 nm. A small fraction of the regenerative amplifier output is focused onto a 5-mm thick CaF_2 crystal to provide an extended visible probe. The pump and probe pulses are focused into spots of ~100 and ~50 μm in diameter, respectively, at the sample position by means of reflective optics in order to avoid degradation of the instrument response function. The resulting pump-probe cross-correlation signal is about 150 fs. The polarization of the pump and probe beam are set at the magic angle (54.7°). After passing through the sample, the probe beam is focused onto the 80-μm input slit of the Triax 190 spectrometer, while using a 300 grooves/mm, 550-nm blaze wavelength grating and focused onto a 1024 pixel CMOS array. Such a configuration allows for a probe window extending from 350 nm to 750 nm with a spectral resolution of 1.3 nm.

Results

At physiological pH, heme f in the cytochrome b_6f complex is fully reduced, while hemes b_p and b_n are fully oxidized, as shown in Figure 3. The heme c_n however has a redox potential of approximately +100 mV, that is in between that of the heme f and the b hemes (+355 mV and -130/-35 mV, respectively[27]). The ratio of oxidized heme c_n is therefore uncertain and any evaluation of this ratio is rendered difficult due to its oxidized minus reduced difference spectrum that is broad and featureless in the spectral window.[27] These broad and featureless spectral features of the heme c_n are on the other hand an advantage as it allows to unambiguously distinguish the signal of the spectrally sharp α-band of the heme f, which is the focus of the present study. The addition of ferricyanide (FeCN) (midpoint potential ≈ +430 mV)[28, 29] effectively oxidizes all hemes (Figure 3).

While trying to access the heme f via excitation of its β-band around 520 nm, the Car and Chl a are predominantly excited. Indeed, even if the main absorbance bands of Car and Chl a are adjacent to this spectral region, most of the underling absorbance at 520 nm is still ascribed to these two pigments (Figure 3). Furthermore, as mentioned above, the reduced heme c_n also absorbs in this spectral region. However, with respect to its spectral features, its signal is expected to be broad, featureless and small compared to that of the heme f. The main task is to differentiate the heme f signal from those of Car and Chl a. In this aim we made use of the redox properties of the heme f, as illustrated in Figure 3:

- In its ferric (oxidized) state, heme f does not show any absorbance band of significant amplitude in the spectral window (450-700 nm), and is consequently found to be unresponsive to laser excitation.
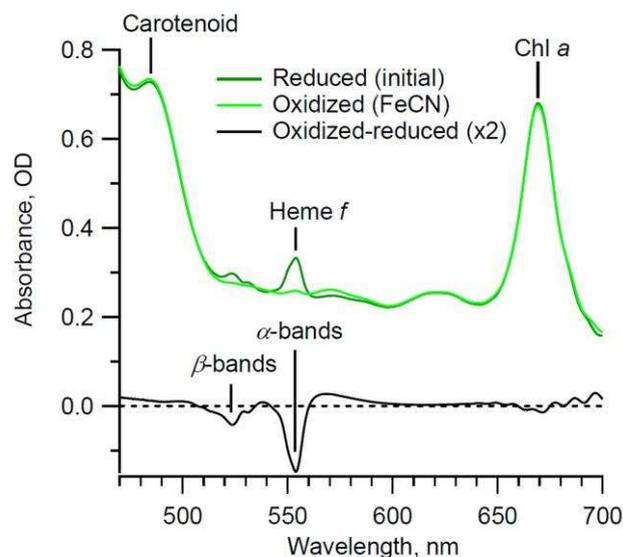
Figure 3: Absorbance spectra of the cytochrome $b6f$ complex in its initial partially reduced state (dark green) and after oxidation by ferricyanide (FeCN) (light green); and their redox difference spectrum (black). The noise above 650 nm (black curve) is associated with the scattering of the probe light passing through the capillary.
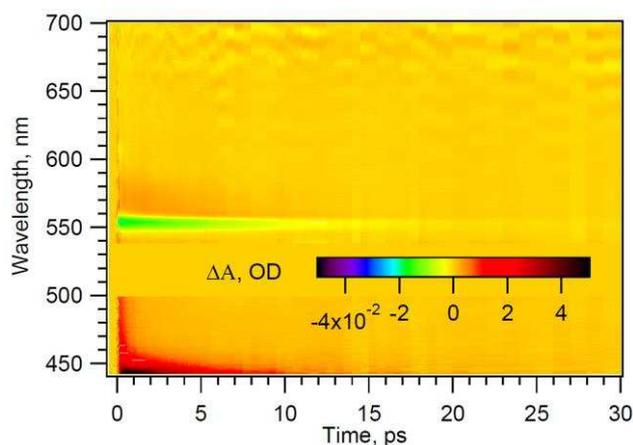
Figure 4: Extracted time-wavelength surface corresponding to the transient absorbance change of the cyt $b6f$ complex excited at 520 nm. The region affected by the pump scattering is set to zero (500-540 nm).

- In its ferrous (reduced) state, however, the heme shows the typical α and β-bands that are responsive to the excitation pulses.

As heme f is situated more than 30Å away from the b hemes, heme c_n, Car and Chl a, it is assumed to be isolated from the dynamics of these chromophores. The spectral signature and photo-induced dynamics of the hemes b and c_n, Car and Chl a are therefore assumed to be unaffected by the oxidation state of heme f and are taken as a background that can be subtracted. The isolated heme f signal is consequently resolved by subtracting the data set corresponding to cyt b_6f complex fully oxidized by FeCN from that of the partially reduced b_6f complex: the heme f is reduced and hemes b are oxidized. The resulting difference signal is shown in Figure 4. The absence of
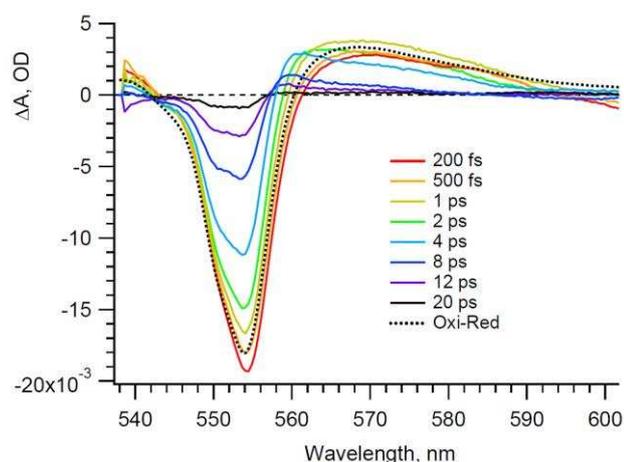
Figure 5: Transient spectra, from the extracted heme *f* signal, measured at multiple time delays. Inset: Transient spectra normalized at 554 nm. The arrows represent the spectral evolution of the signal: a negative and positive lobe appear over time around 550 and 560 nm, respectively. The scaled oxidized minus reduced heme f spectrum is superimposed for comparison only (black dotted line).

a residual signal remaining from the much stronger Car around 580 nm or from Chl *a* in the 670 nm region (Figure 4) indicates the effectiveness of the data treatment. The initial (raw) data is shown in the Supplementary Information (SI, Figure S1). In order to resolve of the evolving heme *f* signal, a selection of transient spectra taken at different time delays is shown in Figure 5. While the spectra measured at short times correspond to the bleach of the heme *f* α-band, those measured at later times differ significantly in that a doublet structure with maxima at 551 and 553 nm appears. The spectral dynamics allude to multiple concomitant relaxation routes. In order to deconvolute the different processes involved in the heme *f* dynamics, the data set is analysed by global fit of selected kinetics, as shown in Figure 6. The data set is satisfactorily fit with a minimum of 3 exponential components.

The heme *f* signal is analyzed via Singular Value Decomposition (SVD). The resulting Decay Associated Spectrum (DAS) is shown in Figure 7. The same exponential decay components are used to adequately fit both the kinetics from Figure 6 and the resulting Eigen-kinetics from the SVD analysis.

While the 420 fs DAS component is characterized by a broad negative featureless signal, the 2.1 and 5.7 ps DAS are characterized by sharp features in the heme *f* α-band region. Despite the fact that none of these DAS can be directly compared to the oxidized minus reduced heme *f* difference spectrum, the sum of the 2.1 and 5.7 ps DAS results in a spectrum that compares well with it. We deduce that the signal generated in 2.1 ps (represented by the 2.1 ps DAS component, Figure 7) decays concomitantly with the bleach signal that resembles the heme *f* oxidized minus reduced difference spectrum, in 5.7 ps.

The 2.1 ps DAS component has a bimodal feature with a zero-crossing point near the heme absorbance maximum, which is typical of a band shift. As no other absorbance band besides those of heme *f* are present in this spectral region, this 2.1 ps
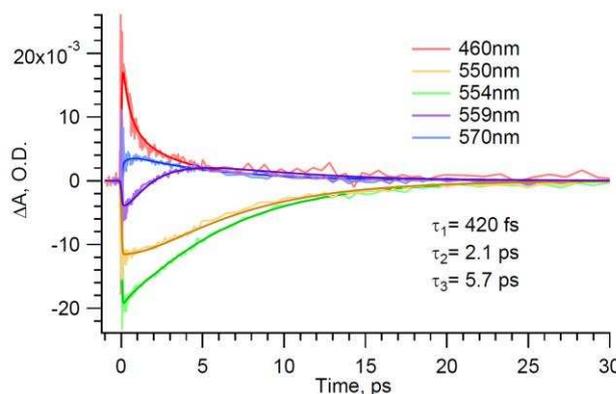
Figure 6: kinetics of the heme *f* and their global fit (smoothed lines) with a satisfactory minimum of three exponential decay components with time constants shown in figure.
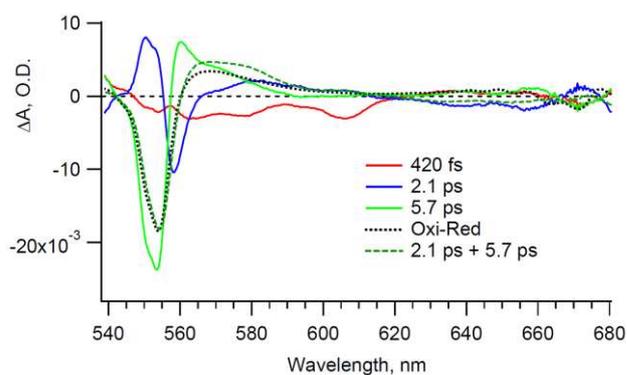
Figure 7: DAS resulting from the SVD analysis of the heme f transient signals. The sum of the 2.1 and 5.7 ps DAS components is shown (green dashed line) and is compared to the scaled oxidized minus reduced heme *f* difference spectrum (black dotted line), shown for comparison.

DAS is assigned to the shift of the heme *f* α-band. It is noted that the SVD analysis, by definition, is limited when it comes to resolving gradual spectral changes that do not implicate specific spectral species and clear deconvolution of the signals requires a complementary fitting procedure. In order to verify the hypothesis of a band shift, and to better understand the nature and the evolution of this shift, the heme *f* region is fit at each time delay with the heme *f* oxidized minus reduced spectrum difference superimposed with a reconstructed shift of the same band. The underlying assumption is that the heme whose band is shifted retains both its coordination and reduction state; in other words, the heme *f* remains ferrous and 6-coordinated. The amplitude of the oxidized minus reduced band (A_b), the amplitude of the band responsible for the shift (A_s) and the magnitude of the shift (S) are kept as free parameters. Examples of the fits are shown in Figure 8. Further details of the fitting procedure as well as the quality of the fits are presented in the SI.
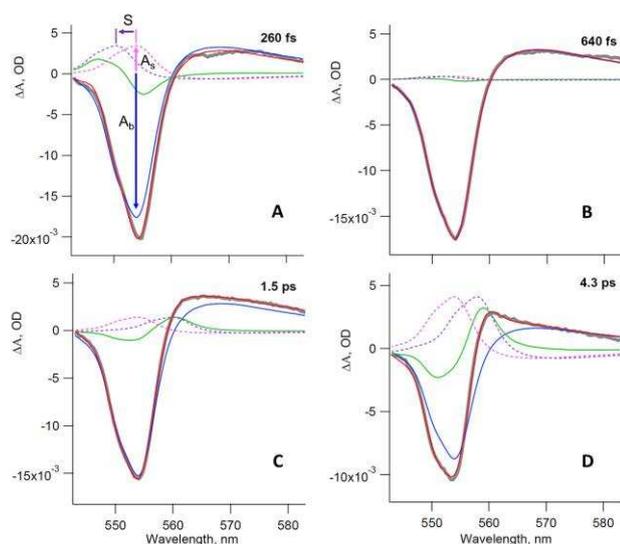
Figure 8: Fitting results at 260 fs (A), 640 fs (B), 1.5 ps (C) and 4.3 ps (D). The fit (red curves) to the data (gray curves) consists of the oxidized minus reduced spectrum of heme *f* (blue curves) and the heme *f* band shift (green curves). The band shift itself is the difference between the fixed heme *f* reduced minus oxidized spectrum (pink dotted curves) and its shifted duplicate (purple dotted curves). The first panel also includes fitting variables, the amplitude of the oxidized-reduced spectrum (Ab), the amplitude of the band responsible for the shift (As), and the magnitude of the shift (S).
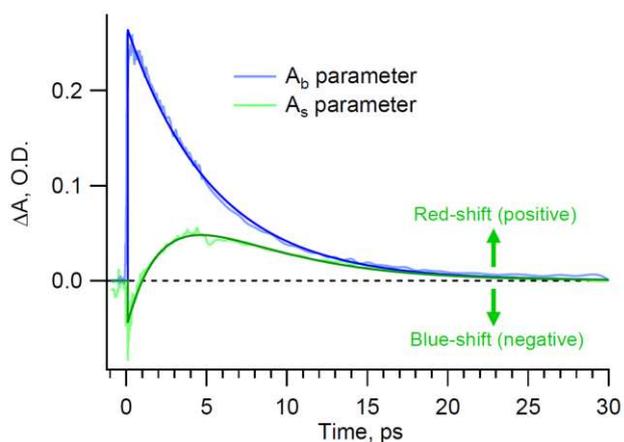
Figure 9: Time evolution of the fitting variables.

The evolution of the principal fitting variables is plotted in Figure 9. The "A$_b$" parameter represents the amplitude of the band responsible for the bleach, while the "A$_s$" parameter corresponds to the amplitude of the band responsible for the shift: negative and positive values indicate a blue and red shift, respectively. The time evolution of the fitting variables are now clearly resolved and are themselves fitted with an adequate kinetic model, as discussed in the next section.

The band-shift magnitude (shown in SI), the "S" parameter, changes progressively from an initial blue-shift of about -3.5 nm, which is "instantaneously" generated, to a red-shift, which reaches a maximum of about +4.5 nm at ~5 ps. The shift then relaxes concomitantly with the heme *f* bleach signal. The origin of the band-shift as well as its possible correlation with the bleach dynamics are also discussed subsequently.

Discussion

Heme photo-dissociation? In order to tentatively assign the different exponential components to particular processes we first investigate the possibility of heme photo-dissociation as it is one of the most common relaxation mechanisms that occur in heme-proteins. The previously studied heme c_1 from the cyt bc_1 complex, which is functionally analogous to heme *f* considered in the present study, was suggested to photo-dissociate one of its ligands,[20] in accordance with previous studies on cyt *c* [18, 19] and a variety of other heme proteins with similar coordination states.[17] Interestingly, the transient signal monitored from heme *f* is clearly different from that of the homologue heme c_1. While the extracted DAS from the heme c_1 in cyt bc_1 [20] and from the cyt *c* analysis[18, 19] were dominated by a broad ESA (positive) signal, the heme *f* analysis results in three DAS that are apparently deprived of any such ESA. In particular, the ~6 ps DAS component, corresponding to the rebinding of the *c*-type heme in cyt bc_1 and cyt *c* with their axial ligand, was characterized by a photo-product (the 5-C species) whose spectrum is red-shifted and much broader than that of the oxidized 6-C species. However, similar signals are not observed for the heme *f*. Furthermore it has been shown via comparative vibrational spectroscopy that the displacement of the heme *f*'s iron center was significantly impaired (compared to that of myoglobin which undergoes photo-dissociation [15]) and that the heme itself was more rigidly entrained by the protein.[30] We consequently do not expect the heme *f* to photo-dissociate with its axial ligand.

Heme photo-oxidation? It is the remarkable quality of the fits in Figure 8 that directs our attention to photo-oxidation being one of the major relaxation pathways, because it uses the reduced minus oxidized heme *f* difference spectrum to reproduce both bleach and shift. Fits of further time delays are shown in SI. Yet photo-oxidation is generally a rare phenomenon in single heme-proteins under visible light excitation.[17] It is however a common occurrence in artificial quinone-substituted porphyrin monomers.[31] These model systems exhibit clear pulse-limited charge separation states with the electron being donated by the porphyrin ring to the covalently bound quinone. The heme *f* in cyt b_6f is also surrounded by aromatic structures: it has a histidine and a tyrosine axial ligand (His-25 and Tyr-1 in the green alga *C. reinhardtii*) [14, 32] and is less than 5 Å away from a tryptophan (Trp 4) and from another tyrosine (Tyr 161) residues (Figure 2). The heme *f* therefore resembles the model systems studied by Rodriguez et al. in that the heme is in close contact (Van der Wall distances) with an aromatic ring. Both Trp and Tyr are known to easily accommodate an extra electron onto their aromatic ring[33] and to effectively serve as electron mediator.[34, 35] In this hypothesis, the heme *f* would undergo a pulse-limited photo-oxidation (i.e. charge separation) with one of the adjacent amino acids. The process which occurs with a life time of 5.7 ps, as resolved by the SVD analysis, thus correspond in part to the subsequent charge recombination (CR) between the ejected electron and the oxidized heme. Using a qualitative approach to the relation between electron

transfer rate and donor-acceptor distance[36]), the distance between the heme and these adjacent amino-acids implies an electron transfer rate of the order of few ps, which is in agreement with this interpretation. Additionally, the presence of aromatic residue 4 (in the present case, Trp-4, Figure 2) in the vicinity of the heme iron center has been proposed to stabilize the oxidized form of the heme via π-based repulsive negative electrostatic interaction with the iron atom.[14] Such electrostatic interaction suggests that if charge separation occurs (photo-oxidization) the oxidized state of the heme is stabilized. The life time of the charge separated state is therefore expected to be in the ps-time range. In light of these arguments we interpret the calculated 5.7 ps from the SVD analysis as being representative of the CR between the photo-oxidized heme iron center and one of the surrounding amino acid, which would then play the role of a transient electron acceptor. However, the band shift implies the presence of additional electronic and nuclear processes.

Heme vibrational relaxation? Beside photo-dissociation, another common route for the heme-protein to relax is via Vibrational Relaxation (VR), or vibrational energy redistribution, as it is the case for cyt c[19] and other porphyrins. This VR typically results in a band shift similar to the one monitored. However, the underlying assumption in such a band-shift is that the heme remains a 6-coordinated ferrous heme.[31] This process is thus parallel or consecutive to the photo-oxidation mentioned in the present study. Rodriguez et al. showed in their quinone-substituted porphyrin model systems that the subsequent CR to the photo-oxidation results in a vibrationally "hot" ground state characterized by a red-shifted spectrum.[31, 37] The excess energy then dissipates via VR and the spectrum blue-shifts to its original position. This mechanism can explain the appearance of the red shift and its relaxation ~5 ps onward. It however does not explain the initial (pulse-limited) shift monitored as the band is initially shifted to the blue (Figure 9). We thus conclude that not all heme f undergoes photo-oxidation and that part of the excited hemes, which still remain in their electronic and coordination states, are rather instantaneously promoted to an (non-dissociative and non-oxidative) excited state. This excited state then relaxes and its transient signal is concomitantly overcome by the red shifted vibrationally hot ground state resulting from the CR pathway.

As mentioned by Rodriguez et al.,[31] it is not trivial to differentiate between intra- and relaxation processes as both can occur on a similar ps time scale. Furthermore, the heme f is covalently attached to the cytochrome backbone and we consequently cannot formally talk about intramolecular or internal vibrational relaxation of the excited heme. Energy transfer from the heme to the surrounding amino acids is then expected and the shifts could readily result from the reorganization of the heme environment rather than from an internal electronic or nuclear modification. Fortunately, both intra and intermolecular vibrational relaxation give rise to band-shifts that are opposite in sign. In general terms, while the blue-shift is representative of a weakening of the guest-host interaction, the red shift is usually representative of an
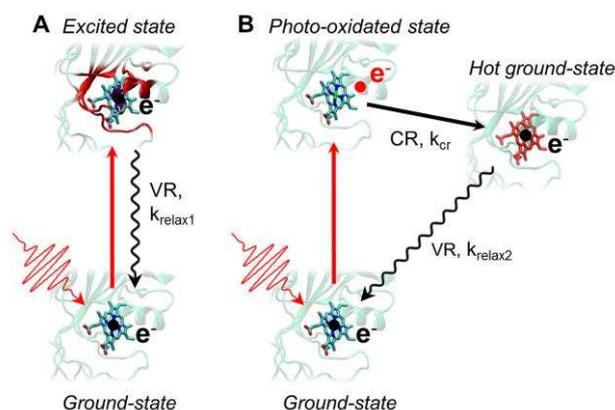
Figure 10: Kinetic model of the two parallel relaxation pathways. Panel A represents the pulse-limited excitation of the ferrous heme that results in the initial blue-shifted signal and its relaxation via Vibrational Relaxation (VR). Panel B shows the pulse-limited photo-oxidation of the heme that result in the bleach signal and its subsequent charge recombination (CR) and cooling via VR that give rise to the red-shift signal and its decay. The decay rates k_{relax1}, k_{cr} and k_{relax2} are used to fit the kinetics of Figure 9. For simplicity and visual purposes, the red-shaded areas represent where most of the energy is expected to reside (in the heme surrounding, within the charge-separated electron or on the heme itself), as discussed in the text.

expansion of the heme macrocycle from a vibrationally excited ground state[31] Interestingly, the data shows both a blue and a red shift. We therefore each shift to specific mechanisms, and propose two parallel mechanisms, as depicted in Figure 10.

In the first scenario, scheme A in Figure 10, the heme could transfer the deposited energy to its environment, i.e. to the surrounding amino acid residues, which would undergo structural rearrangement. It has been shown that the heme f is strongly coupled to the vibrational modes of the protein,[30] which is in agreement with an ultrafast radiationless energy transfer mechanism. In addition, the monitored immediate blue-shift of the band (Figure 9), indicates that this energy transfer is pulse limited. The subsequent excited amino acid residue would in turn affect the heme absorbance spectrum. The magnitude of an electrochromic shift depends directly on the distance and on the relative orientation of the changes in dipole moment of both proteins involved.[38] As the monitored band-shift is relatively large (−3.5 nm initially) and assuming that it is solely due to the conformational changes of the surrounding, the implicated amino acid residue has to be adjacent to the heme and in proper orientation. Such an occurrence is, in fact, common in heme-proteins. In particular, it has been shown that the identity of the aromatic residue 4 in the cyt f subunit does considerably affect the heme f α-band spectrum, up to 2 nm in static measurements, indicating that the heme f's spectrum is affected by this particular residue (Trp 4 in our case).[14] Furthermore, we point out that heme f is ligated with the Tyr-1 residue via the N-terminal (amine group) of the protein rather than with its organic substituent (such as the aromatic ring in the case of His ligation). Displacement of the Trp aromatic ring would therefore not affect the coordination state of the heme but would affect the heme spectrum. It has also been suggested that the heme pocket undergoes structural rearrangement upon redox changes.[39] It

is therefore reasonable to expect structural rearrangement as a result of light excitation.

In the second scenario, scheme B in Figure 10, since a similar red-shift is also seen in free-based (devoid of metal center) single porphyrins,[37] we expect the extra energy to reside on the heme macrocycle. This sudden energy increase would result in a nuclear reorganization of the heme[40] and "stimulate some intra-molecular vibrational activity".[31]

The kinetic model of Figure 10 allows us to refine the different reaction rates by fitting the curves in Figure 9 with the following set of equations:

- The bleach signal (blue curve in Figure 9) is fit as a single exponential representing the CR, with a rate k_{cr}:

$$A_b(t) = A_{b_0} \cdot e^{-k_{cr} \cdot t} \qquad (1)$$

- The shift signal (green curve in Figure 9) is fit as if the initial blue shift originates solely from scheme A and the later red shift is solely due to the relaxation mechanisms of scheme B (Figure 10):

$$A_s(t) = A_{blue-shift}(t) + A_{red-shift}(t) \qquad (2)$$

The blue and red shifts correspond to a first and second sequential reaction, respectively:

$$A_{blue-shift}(t) = A_{s_0} \cdot e^{-k_{relax1} \cdot t} \qquad (3)$$

$$A_{red-shift}(t) = A_{b_0} \cdot \frac{k_{cr}}{(k_{cr} - k_{relax2})} \cdot (e^{-k_{cr} \cdot t} - e^{-k_{relax2} \cdot t}) \quad (4)$$

We find that the relaxation rate from the initially excited state, k_{relax1}, is $(2.5 \text{ ps})^{-1}$, the CR, k_{cr}, is $(5.3 \text{ ps})^{-1}$ and the relaxation of the residual excess vibrational energy, k_{relax2}, is $(3.6 \text{ ps})^{-1}$. Note that the initial excitation is taken as being "instantaneous" (a Dirac function) since it is faster than our time resolution of ~100 fs. In either case, whether the heme structure is directly modified (scheme B) or the heme spectrum is simply affected by the reorganization of its surroundings (scheme A), it is interesting that both relaxations are fast with a life time of about 3 ps. From the initial amplitudes A_{b0} and A_{s0} of our simplified model (Equation 1-4), we infer that about 85 % of the excited hemes undergo photo-oxidation (scheme B), while the remaining 15 % follow a non-dissociative, non-oxidative relaxation pathway (scheme A).

Contribution of heme c_n? Concerning the 420 fs component resulting from the global fit and SVD analysis, it is important to note that it differs from the sub-ps components monitored in the photo-oxidation of the hemes b in the homologue cyt bc_1 complex. Our 420 fs DAS component is not characterized by any sharp features resembling that of the α-band spectrum. It also differs from the broad and featureless excited state absorption signal that is anticipated if the heme would photo-dissociate, as it is negative. Indeed, a negative feature in transient absorption can only be assigned to bleaching or to a stimulated emission (SE) signal. Both a bleach and SE signal from the heme f are expected to be spectrally characterized by a sharp α-band-like signal. This broad and featureless spectrum is on the other hand characteristic of either the ferric
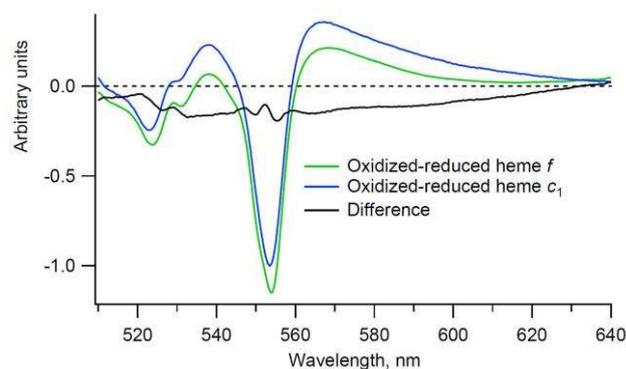
Figure 11: Reduced minus oxidized spectrum of heme f from cyt b_6f (green) superimposed with that of the heme c_1 from cyt bc_1 (blue). Their amplitude has been adjusted to have similar α-band magnitude. The difference spectrum is shown in black.

heme f or of the ferrous heme c_n.[27] However, it has been shown in the cyt bc_1 complex that the ferric state of the heme b was not responsive to similar laser excitation.[20] We therefore do not expect the ferric heme f to yield any strong signal. Due to the redox potential of the heme c_n, which is approximately +100 mV,[27] it is possible that a fraction of these hemes were initially in their ferrous state, as previously mentioned. In order to verify this hypothesis we compared the static spectrum of the heme f with that of its homologue, the heme c_1 form the cyt bc_1. Shown in *Figure 11* are the two hemes, which, despite their distinct structure, are very similar. The difference spectrum between the two species is characterized by a broad and featureless band that corresponds in parts to the previously reported reduced minus oxidized (i.e., ferrous) heme c_n.[27]

The presence of ferrous heme c_n implies that it is absorbing part of the excitation energy and it can be expected to bleach. Ultrafast electronic relaxation of these excited hemes c_n would then give rise to a transient signal that corresponds to our monitored 420 fs DAS component seen in *Figure 7*, i.e. to a broad and featureless negative band. However, the precision of the data at early delay times does not allow for further analysis. Complementary fluorescence and Raman analysis would help in better understanding the data and are underway. Furthermore, due to the distance separating heme f and c_n, the dynamics of the two hemes are assumed to be independent and we emphasize that such possible participation of the heme c_n does not influence the heme f analysis, which is the focus of this paper.

Mechanistic consequences. The behavior of the heme f from cyt b_6f differs significantly from that of its homologue heme c_1 from cyt bc_1. It was concluded that it is the unique structure of the protein that dictates heme f's unique behavior: While the axial ligand to heme c_1 was found to photo-dissociate, the heme f apparently photo-oxidizes and undergo structural reorganization that leads to a substantial band-shifts. Though different in their structure and in their ultrafast relaxation mechanisms, both the heme f from the cyt b_6f and the heme c_1 from the cyt bc_1 complexes serve similar physiological purposes.[41, 42] The present study thus shows that none of the ultrafast behavior, i.e. photo-oxidation, photo-dissociation and

structural rearrangement, is a limiting factor to the overall electron transport and energy transduction mechanisms of the protein that occur on a much longer time scale. With the aim of linking the ultrafast behavior of the heme to the physiological functions, our attention is then directed to the protein backbone rather than to the heme itself. Indeed, since both the heme f and the heme c_1 are believed to mediate electron transfer to the Rieske 2Fe-2S protein complex via a series of conformational changes,[41] the flexibility of the overall subunit and in particular that of the heme binding pocket, might have a role to play in this electron transfer. It was also suggested in a previous Raman analysis "that the cytochrome f heme pocket may undergo structural rearrangement during the redox changes, resulting in a change in the exposure to the solvent for different edges of the heme center".[43] This Raman study implies a certain flexibility of the structure. The monitored band-shift in our analysis supports and extends this conclusion by demonstrating that structural modification can be ultrafast and stabilized within ps. As discussed above, a significant band-shift requires specific molecular arrangements and it is possible that similar structural relaxation processes occur in the homologous heme c_1, while leaving the heme spectrum unchanged. It would then be interesting to investigate what role ultrafast reorganization of the heme binding-pocket has to play in the larger physiological processes of the protein.

Another similarity between the hemes f and c_1 is the apparent lack of response of the ferric species to visible light excitation. This "inactive" state is certainly due to the much weaker absorbance of the ferric species compared to the distinct α-band of the ferrous state. Note that in either case, ferric or ferrous, the most intense absorption band (~400 nm) remains nearly as intense. It would then be interesting to compare the heme responses in the ferric and ferrous state to near-UV excitation.

Finally, we point out the consistence in recovery life time between the different hemes in the cyt bc_1, cyt b_6f, and other heme proteins such as cyt c, myoglobin, etc. Indeed, beside the distinct ultrafast (fs-ps) relaxation mechanisms that take place, it seems that, as long as no exogenous ligands are involved, the ferrous 6-C heme proteins are able to fully recover from light excitation within tenths of pico-seconds. The ability of the hemes to recover on a short time-scale illustrates the general robustness of the embedded hemes in response to light excitation.

Conclusions

The response of the ferrous heme f of the cyt b_6f complex, to 520 nm laser excitation, is monitored via its characteristic α-band. The ability to chemically control the redox state of the heme enables extraction of its signal from the Chl a and Car signals of much larger amplitude. The combination of global fitting procedures with careful frame-by-frame analysis of the data allowed to clearly resolve the overall and gradual spectral changes that are taking place within the heme f. The analysis of the heme ultrafast dynamics shows that about 85 % of the reacting hemes f undergo pulse-limited photo-oxidation (< 100 fs), with the electron acceptor most probably being one of the adjacent aromatic amino acid residues. After charge recombination in 5.3 ps, the residual energy is dissipated in 3.6 ps. In a parallel pathway the remaining 15 % of the hemes directly relax from the excited sate in 2.5 ps. Both excited states give rise to significant opposite spectral band-shifts.

In comparison to the photo-dissociation of heme c_1 of the homologous cyt bc_1 complex, there is no evidence that the heme f also photo-dissociates from its axial ligand. The unusual ultrafast response of the heme f is solely attributed to its specific environment and more specifically to the unusual tyrosine axial ligand. As both species, cyt b_6f and cyt bc_1 complexes, are performing very similar physiological role, we conclude that neither the photo-dissociation nor photo-oxidation are instrumental or detrimental to the overall functions of the proteins.

Furthermore, this study, by the fact that it uses microfluidic technologies and complementary analytical methods, opens the door to a broad range of multiheme proteins that were up to now not suitable for ultrafast spectroscopic investigation. In comparison to other heme-proteins, heme f is a remarkable example of unusual ultrafast physical response and as such illustrates the strong dependence between heme behavior and structural environment.

ACKNOWLEDGMENT

ABBREVIATIONS

Car, β-carotene; Chl a, Chlorophyll a; CN-PAGE, clear native SDS polyacrylamide gel electrophoresis; CR, charge recombination; Cyt, cytochrome; DAS, Decay Associated Spectrum; ESA, Excited State Absorption; FeCN, ferricyanide; n, p, electrochemically negative and positive side of the membrane; VR, vibrational relaxation; SVD, Singular Value Decomposition; UDM, undecyl maltoside.

Notes and references

1. W. A. Cramer, H. Zhang, J. Yan, G. Kurisu and J. L. Smith, *Annu. Rev. Biochem.*, 2006, **75**, 769-790.
2. D. Xia, L. Esser, M. Elberry, F. Zhou, L. Yu and C.-A. Yu, *J. Bioenerg. Biomembr*, 2008, **40**, 485-492.
3. C. Lange and C. Hunte, *Proc. Nat. Acad. Sci. USA*, 2002, **99**, 2800-2805.
4. E. Yamashita, H. Zhang and W. A. Cramer, *J. Mol. Biol.*, 2007, **370**, 39-52.
5. Z. Zhang, L. Huang, V. M. Shulmeister, Y.-I. Chi, K. Kyu Kim, L.-W. Hung, A. R. Crofts, E. A. Berry and S.-H. Kim, *Nature*, 1998, **392**, 677-684.
6. S. S. Hasan, J. T. Stofleth, E. Yamashita and W. A. Cramer, *Biochemistry*, 2013, **52**, 2649-2654.
7. D. Stroebel, Y. hoquet, J.-L. Popot and D. Picot, *Nature*, 2003, **426**, 413-418.

8   G. Kurisu, H. Zhang, J. L. Smith and W. A. Cramer, *Science*, 2003, **302**, 1009-1014.
9   A. I. Zatsman, H. Zhang, W. A. Gunderson, W. A. Cramer and M. P. Hendrich, *J. Am. Chem. Soc.*, 2006, **128**, 14246-14247.
10 S. S. Hasan, E. Yamashita, D. Baniulis and W. A. Cramer, *Proc. Nat. Acad. Sci. USA*, 2013, **110**, 4297-4302.
11 N. Dashdorj, H. Zhang, H. Kim, J. Yan, W. A. Cramer and S. Savikhin, *Biophys. J.*, 2005, **88**, 4178-4187.
12 P. Zuo, B.-X. Li, X.-H. Zhao, Y.-S. Wu, Ai, X.-C., J.-P. Zhang, L.-B. Li and T.-Y. Kuang, *Biophys. J.*, 2006, **90**, 4145-4154.
13 S.-O. Wenk, D. Schneider, U. Boronowsky, J. C., C. Klughammer, F. L. de Weerd, H. van Roon, F. J. Vermaas, J. P. Dekker and M. Rögner, *FEBS J.*, 2005, **272**, 582-592.
14 M. V. Ponamarev, B. G. Schlarb, C. J. Howe, C. J. Carrell, J. L. Smith, D. S. Bendall and W. A. Cramer, *biochemistry*, 2000, **39**, 5971-5976.
15 C. Consani, G. Auböck, O. Bräm, F. van Mourik and M. Chergui, *J. Chem. Phys.*, 2014, **140**, 025103.
16 M. Chergui, in *Comprehensive Biophysics*, ed. E. H. Egelman, Oxford: Academic Press, 2012, vol. 1, pp. 398-424.
17 M. H. Vos, A. Battistoni, C. Lechauve, M. C. Marden, L. Kiger, A. Desbois, E. Pilet, E. de Rosny and U. Liebl, *Biochemistry*, 2008, **47**, 5718-5723.
18 C. Consani, O. Bräm, F. van Mourik, A. Cannizzo and M. Chergui, *Chem. Phys.*, 2012, **396**, 108-115.
19 W. Wang, X. Ye, A. A. Demidov, F. Rosca, T. Sjodin, W. X. Cao, M. Sheeran and P. M. Champion, *J. Phys. Chem. B*, 2000, **104**, 10789-10801.
20 A. A. P. Chauvet, A. Al Haddad, W.-C. Kao, F. Van Mourik, C. Hunte and M. Chergui, *Phys. Chem. Chem. Phys.*, 2014.
21 M. Negrerie, S. Cianetti, M. H. Vos, J.-L. Martin and S. G. Kruglik, *J. Phys. Chem. B*, 2006, **110**, 12766-12781.
22 D. Baniulis, H. Zhang, T. Zakharova, S. S. Hasan and W. A. Cramer, in *Photosynthesis Research Protocols, Methods in Molecular Biology*, ed. R. Carpentier, Springer Science, 2011, vol. 684.
23 H. Zhang, J. P. Whitelegge and W. A. Cramer, *J. Biol. Chem.*, 2001, **276**, 38159-38165.
24 A. Chauvet, T. Tibiletti, S. Caffarri and M. Chergui, *Rev. Sci. Instrum.*, 2014, **85**.
25 A. Lisibach, E. Casartelli and N. Schmid, ASME 2010 3rd Joint US-European Fluids Engineering Summer Meeting and 8th International Conference on Nanochannels, Microchannels, and Minichannels, Montreal, Quebec, Canada, 2010.
26 J. Helbing, L. Bonacina, R. Pietri, J. Bredenbeck, P. Hamm, F. van Mourik, F. Chaussard, A. Gonzalez-Gonzalez, M. Chergui, C. Ramos-Alvarez, C. Ruiz and J. López-Garriga, *Biophys. J.*, 2004, **87**, 1881-1891.
27 J. Alric, Y. Pierre, P. Picot, J. Lavergne and F. Rappaport, *Proc. Nat. Acad. Sci. USA*, 2005, **102**, 15860-15865.
28 M. Pandurangachar, B. E. Kumara Swamy, B. N. Chandrashekar, O. L. Gilbert, S. Reddy and B. S. Sherigara, *Int. J. Electrochem. Sci.*, 2010, **5**, 1187-1202.
29 M. E. Girvin and W. A. Cramer, *Biochim. Biophys. Acta*, 1984, **767**, 29-38.
30 K. L. Adams, S. Tsoi, J. Yan, S. M. Durbin, A. K. Ramdas, W. A. Cramer, W. Sturhahn, E. E. Alp and C. Schulz, *J. phys. Chem. B*, 2006, **110**, 530-536.
31 J. Rodriguez, C. Kirmaier and D. Holten, *J. Phys. Chem.*, 1991, **94**, 6020-6029.
32 W. A. Cramer, G. M. Soriano, M. Ponomarev, D. Huang, H. Zhang, S. E. Martinez and J. L. Smith, *Annu. Rev. Plant Physiol. Plant Mol. Biol.*, 1996, **47**, 477-508.
33 R. A. Malak, Z. Gao, J. F. Wishart and S. S. Isied, *J. Am. Chem. Soc.*, 2004, **126**, 13888-13889.
34 H. B. Gray and J. R. Winkler, *B. B. A. - Bioenergetics*, 2010, **1797**, 1563-1572.

35 H. B. Gray and J. R. Winkler, *Proc. Nat. Acad. Sci. USA*, 2015, **112**, 10920-10925.
36 C. C. Moser, J. M. Keske, K. Warnck, R. S. Farid and P. L. Dutton, *Nature*, 1992, **355**, 796-802.
37 J. Rodriguez, C. Kirmaier, M. R. Johnson, R. A. Friesner, D. Holten and J. L. Sessler, *J. Am. Chem. Soc.*, 1991, **113**, 1652-1659.
38 N. Dashdorj, W. Xu, P. Martinsson, P. R. Chitnis and S. Savikhin, *Biophys. J.*, 2004, **86**, 3121-3130.
39 F. Gao, H. Qin, M. C. Simpson, J. A. Shelnutt, D. B. Knaff and M. R. Ondrias, *Biochemistry*, 1996, **35**, 12812-12819.
40 T. G. Spiro, J. D. Stong and P. Stein, *J. Am. Chem. Soc.*, 1979, **101**, 2648-2655.
41 E. A. Berry, M. Guergova-Kuras, L. Huang and A. R. Crofts, *Annu. Rev. Biochem.*, 2000, **69**, 1005-1075.
42 W. A. Cramer, S. S. Hasan and E. Yamashita, *B. B. A. - Bioenergetics*, 2011, **1807**, 788-802.
43 F. Gao, H. Qin, D. B. Knaff, L. Zhang, L. Yu, C.-A. Yu, K. A. Gray, F. Daldal and M. R. Ondrias, *Biochim. Biophys. Acta*, 1999, **1430**, 203-213.